

ENGINEERING RESEARCH INSTITUTE
UNIVERSITY OF MICHIGAN

ATMOSPHERIC PHENOMENA AT HIGH ALTITUDES

Department of the Army
Contract No. DA-36-039 SC-15443
(Meteorological Branch, Signal Corps)

Progress Report No. 5 Quarterly Report

for the period

January 1, 1953 to March 31, 1953

Department of the Army Project No. 3-99-07-22
Signal Corps Project No. 172B

Submitted for the project by:

L. M. Jones

UNIVERSITY OF MICHIGAN PROJECT PERSONNEL

Both Part Time and Full Time

Ammerman, William L., Laboratory Assistant
Bartman, Fred. L., M.S., Research Engineer
Chaney, Lucian W., B.S., Research Engineer
Filsinger, Edward A., Machinist
Gleason, Kermit L., Machinist
Hansen, William H., B.S., Research Associate
Harrison, Lillian M., Secretary
Jones, Leslie M., B.S., Project Supervisor
King, Jay B., B.A., Research Associate
Liu, Vi Cheng, Ph.D., Research Engineer
Loh, Leslie T., M.S., Chemist
Nichols, Myron H., Ph.D., Prof. of Aero. Eng.
Pattinson, Theodore R., Electronic Technician
Samborski, Cassimere, Machinist
Schaefer, Edward J., M.S., Research Engineer
Titus, Paul A., Research Technician
Wenk, Norman J., B.S., Research Engineer
Wenzel, Elton A., Research Associate

TABLE OF CONTENTS

<u>Section</u>	<u>Topic</u>	<u>Page</u>
1.	INTRODUCTION	1
2.	SUMMARY	1
3.	SPHERE EXPERIMENT	1
	3.1 SC-23	1
	3.2 Sphere Drag Coefficients	5
	3.3 SC-29	7
	3.4 SC-30	7
	3.4.1 Design	7
	3.4.2 Ejection Test	11
	3.4.3 Electronics	13
	3.5 Large Sphere for Measuring Winds	18
	3.6 References	20
4.	SAMPLING	21
	4.1 Sample Analysis	21
	4.2 Sampling Aerobee SC-31	21
	4.3 Miscellaneous	25
	4.4 References	25
5.	CORRECTION	26
6.	REPORTS ISSUED AND LABORATORIES VISITED	26
7.	FUTURE PROGRAM	26
8.	ACKNOWLEDGMENT	26

ILLUSTRATIONS

<u>Figure No.</u>	<u>Title</u>	<u>Page</u>
1	Density vs. Altitude, SC-23	3
2	Temperature vs. Altitude, SC-23	4
3	Sphere Drag Coefficients, Isometric Plot	5
4	Sphere Drag Coefficients, Navord Report 2352	6
5	Ejection System, SC-30	8
6	Sling-Shot Ejector, SC-30	9
7	Fiberglas Cord Tie-Down Detail and Blasting Cap "Gun," SC-30	9
8	Hold-Down Lever for Sphere Evacuation Valve, SC-30.	10
9	Revised Sphere Inflation Valve, SC-30	10
10	Test Set-Up, Wright Field, SC-30	11
11	Sphere Ejection and Inflation, SC-30	12
12	Sphere and Chamber Pressures, Ejection Test, SC-30	12
13	Sphere and Internal Cylinder Pressures, Ejection Test, SC-30	13
14	Spin Ambiguity of Crossed-Loop Antennas	14
15	Single Doppler Antenna, SC-30	17
16	Large-Sphere Trajectory	19
17	Sampling Aerobee SC-31	22
18	Seals in 2-Inch Copper Tube	23
19	The 2-Inch Pyrotechnic Sealer for Flight, SC-31	24
20	Pictures Taken with Robot-Star Camera	24

ATMOSPHERIC PHENOMENA AT HIGH ALTITUDES

Department of Aeronautical Engineering

1. INTRODUCTION

This is the fifth in a series of quarterly reports on Contract No. DA-36-039 SC-15443 describing high-altitude meteorological experiments being carried out by the University of Michigan for the Meteorological Branch of the Signal Corps. This program is a continuation of one which was carried out between July 1946 and August 1950 on Contract No. W-36-039 sc-32307 and from August 1950 to December 1951 on Contract No. DA-36-039 sc-125. For background material the reader is referred to the final reports on these contracts and the previous ones of this series.

2. SUMMARY

The work during the first quarter of 1953 was devoted to the reduction of data from sphere Aerobee SC-23, the design of sphere Aerobee SC-30 to be fired 15 April, the study of possible causes of separation in rocket samples, and the planning of sampling Aerobee SC-31 to be fired in the summer of 1953.

3. SPHERE EXPERIMENT

3.1 SC-23

Sphere Aerobee SC-23 was fired on 14 May 1952 as described in Progress Report No. 2. Since then the doppler count, spin correction, and trajectory calculations were completed by Ballistic Research Laboratories. The final data from which density and temperature are calculated were presented in the form of X, Y, Z position coordinates of the sphere in feet, measured with respect to a transverse mercator coordinate system with the origin at the Aerobee launcher. Points were tabulated for each half-second interval of time. In this form the data are "raw," the spin correction being primarily a real correction with only minor smoothing. Several methods of calculating velocities, accelerations, densities, and temperatures were used as well as various methods of smoothing. A comparison of the final density values obtained from the various methods showed agreement within experimental error.

Fig. 1 is a plot of density vs. altitude over the interval from 217,000 feet to the point where the doppler unit left the sphere at 117,000 feet. Also shown in Fig. 1 is a plot of the UARRP atmosphere¹ density values for comparison. The calculations of the sphere points were made as follows:

- 1) The raw position data were differentiated twice by taking first and second differences per half second.
- 2) The second difference accelerations were then smoothed by progressive averaging over 8-second intervals.
- 3) Densities were calculated using the drag equation. C_D values were chosen with Reynolds numbers and Mach numbers as parameters based on UARRP atmosphere values of density and temperature. These values could have been estimated and corrections made by successive approximations without the use of UARRP values.

At this point the telescope tracking film of the sphere was very carefully examined. It was definitely determined that the sphere collapsed at 214 seconds or 167,000 feet. It was decided to do nothing further with the data below this altitude.

Although densities obtained by various methods of treating the data were in satisfactory agreement, the small differences caused fairly large differences in the calculated temperatures because of the sensitivity of the temperature-density function. In order to avoid introducing scatter due to the method of reducing the data, calculations of temperature were made using the raw unsmoothed trajectory data. A plot of these values is shown in Fig. 2 where the results are again compared with the UARRP atmosphere. In Fig. 2 are also shown: a) the error in temperature due to a ± 0.1 -cycle-per-half-second error in counting the doppler cycles, and b) a parabola fitted by least squares to the temperature points. It is current practice to count doppler cycles to ± 0.1 cycle per half second even though with some additional effort cycles could be counted to perhaps ± 0.01 cycle per half second. The ± 0.1 -cycle-per-half-second precision was chosen as being that precision which would result in an error smaller than errors due to other causes such as errors in the station survey, error in the velocity of propagation, and residual error in the spin correction. It was thought that the latter error would be the largest, perhaps four times the count error. It is interesting to note, however, in Fig. 2 that the points lie within the counting error band even though they include scatter due to the spin error. It is also seen in Fig. 2 that the temperature is in good agreement with the UARRP average temperature.

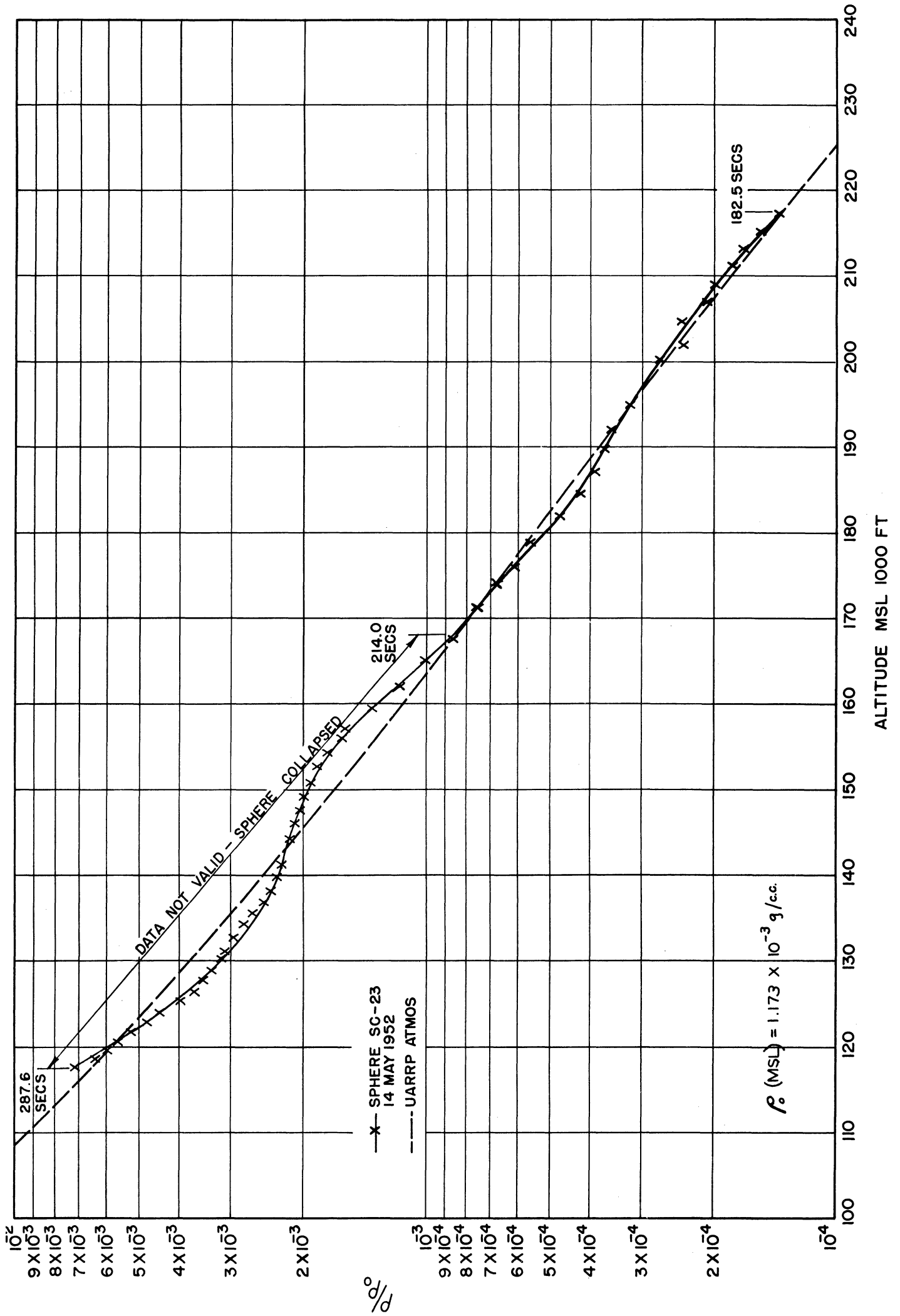
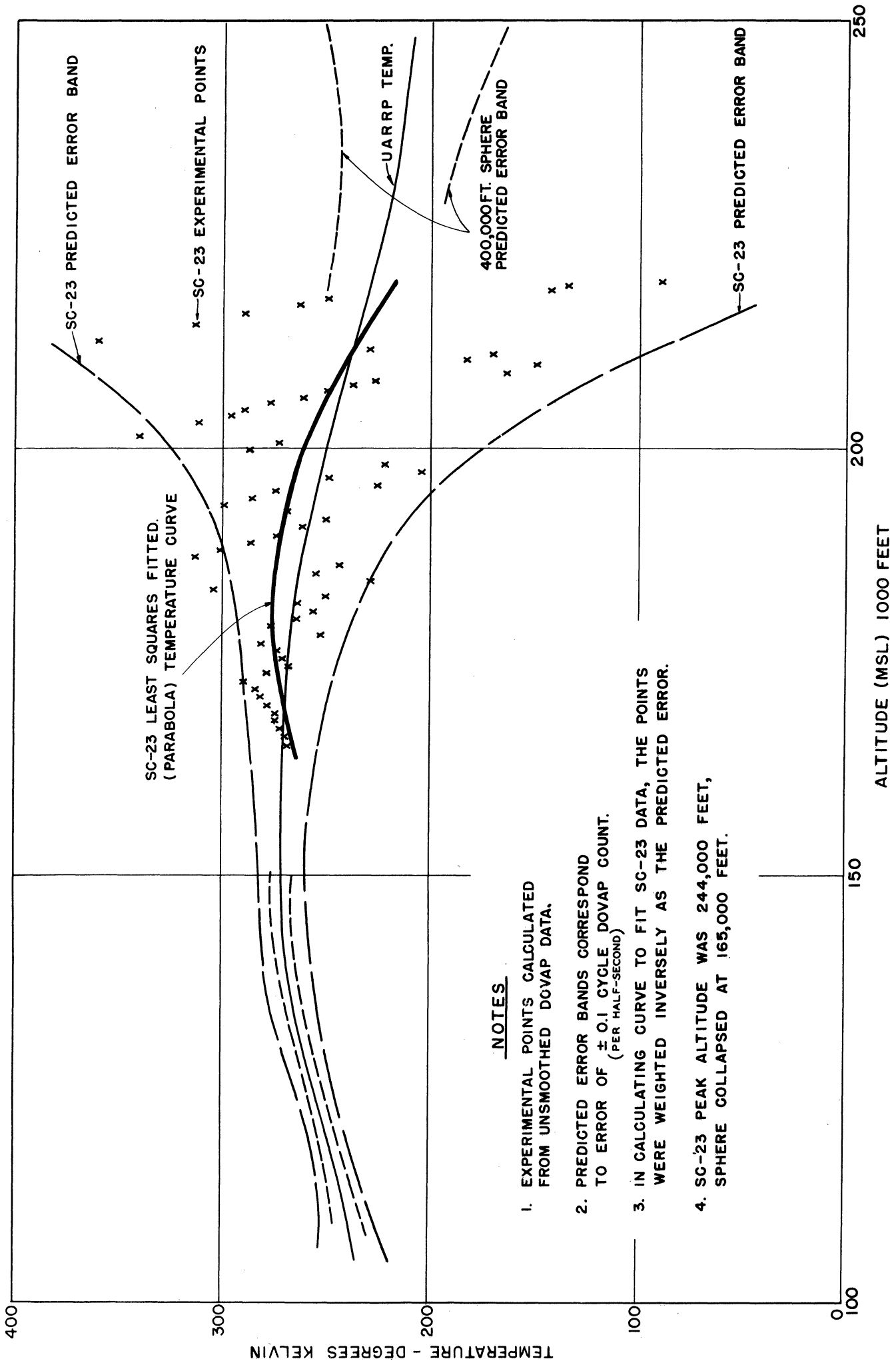


Fig. 1. Density vs. Altitude, SC-23.



NOTES

1. EXPERIMENTAL POINTS CALCULATED FROM UNSMOOTHED DOVAP DATA.
2. PREDICTED ERROR BANDS CORRESPOND TO ERROR OF ± 0.1 CYCLE DOVAP COUNT. (PER HALF-SECOND)
3. IN CALCULATING CURVE TO FIT SC-23 DATA, THE POINTS WERE WEIGHTED INVERSELY AS THE PREDICTED ERROR.
4. SC-23 PEAK ALTITUDE WAS 244,000 FEET, SPHERE COLLAPSED AT 165,000 FEET.

Fig. 2. Temperature vs. Altitude, SC-23.

3.2 Sphere Drag Coefficients

In response to a request by the Engineering Research Institute of the University, a program of measuring the drag coefficients of spheres was undertaken at the U. S. Naval Ordnance Laboratory, White Oak, Maryland. The results of this work have been reported from time to time in previous progress reports. A complete report by NOL² was received. The results of these measurements and similar ones by other investigators are given in Fig. 3 of the NOL report. As an aid to visualizing the C_D surface, an isometric plot was prepared; it is seen in our Fig. 3 below. Fig. 4 is a reproduction of the results as shown in Fig. 3 of the NOL report.

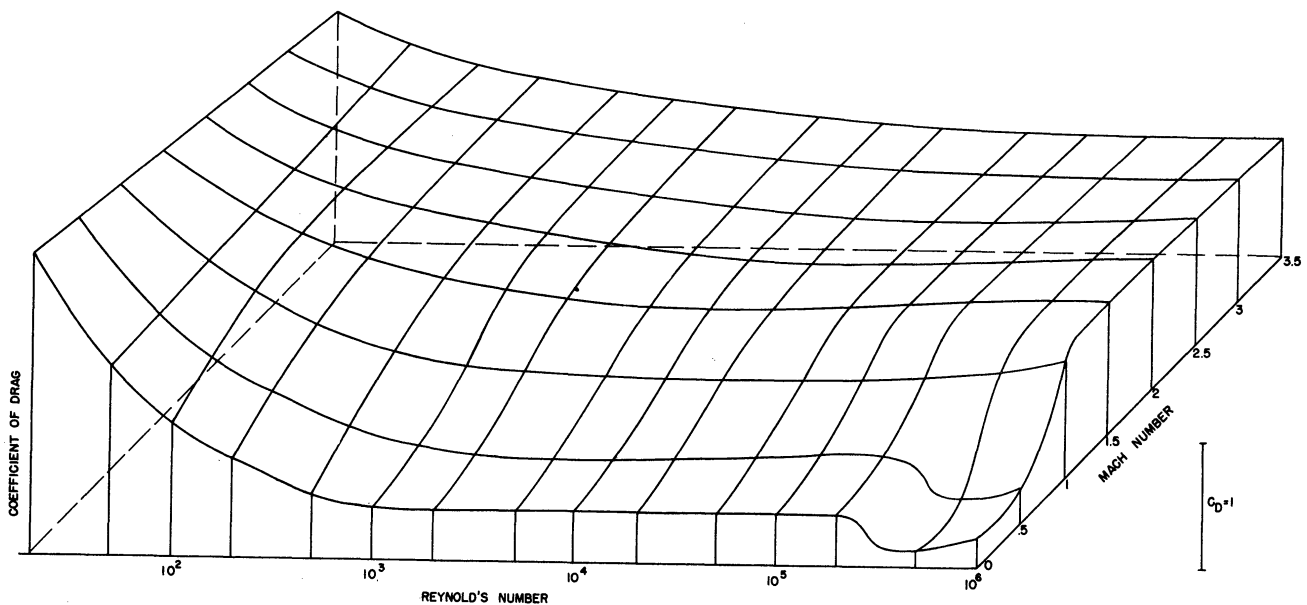


Fig. 3. Sphere Drag Coefficients, Isometric Plot.

CONTOUR MAP OF DRAG COEFFICIENT AS A FUNCTION OF MACH NUMBER AND REYNOLDS NUMBER

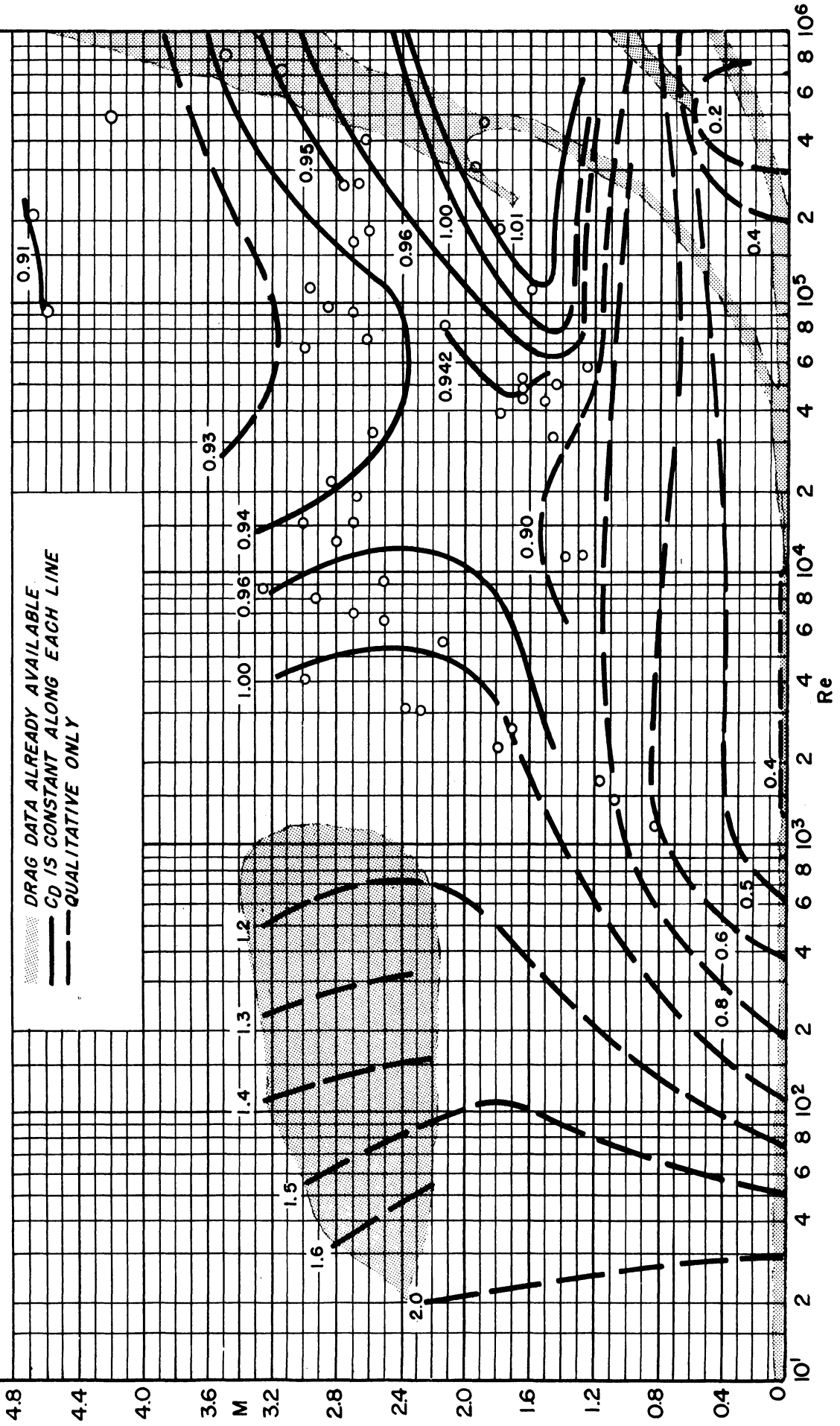


Fig. 4. Sphere Drag Coefficients, Navord Report 2352.

3.3 SC-29

The reduction of data from SC-29, fired on 11 December 1952, was started by Ballistic Research Laboratories.

3.4 SC-30

3.4.1 Design

Preparation of a third sphere Aerobee SC-30 was begun. The firing was scheduled for 15 April. A new ejection system, shown in Fig. 5, was designed, constructed, and tested. In this design, the sphere is contained in a continuous 15-inch diameter cylinder of Textolite. The lower access door rests on a ring which together with 6 rubber bands 1/8 inch x 1-1/2 inches comprises a large sling shot. The bands pass vertically between the collapsed sphere and outer cylinder through slots in the outer cylinder to which they are clamped on the outside. The bands are approximately 12 inches long and are stretched to 48 inches. The sphere is held in place and the bands held stretched by the nose cone, which in turn is held down by a Fiberglas cord passing through the base of the nose cone and down the outside of the cylinder. The cord is clamped to the base of the cylinder. Just above the clamps on either side is a steel "gun," each containing two blasting caps. Near the peak of the trajectory the blasting caps are fired by doppler command, thus severing the glass cord. This releases the nose cone and permits ejection of the sphere by the sling shot. To permit evacuation of the sphere during ascent, it is provided with a spring-operated valve which is held open by a lever which in turn is held depressed by the glass cord. When the cord is severed the lever lifts, allowing the valve to close.

In order to insure that the sphere is completely ejected before inflation starts, the inflation valve (described in a previous report) is fitted with a dash-pot having a three-second delay. The sphere for SC-30 differs in only one other particular from the one in SC-29: The access door rings to which the gores are attached are made of solid nylon of the same composition as the sphere fabric. This permits a hot-seal joint instead of a cemented joint, resulting in greater strength, smoothness, and flexibility.

Fig. 6 shows the sling-shot ejector, Fig. 7 the details of the Fiberglas tie-down cord with the "gun" which contains the blasting caps for severing the cord. Fig. 8 shows the lever which holds open the sphere evacuation valve and the Fiberglas cord holding the lever in flight position. Fig. 9 is a drawing of the revised sphere inflation valve with the dash-pot for providing a time delay.

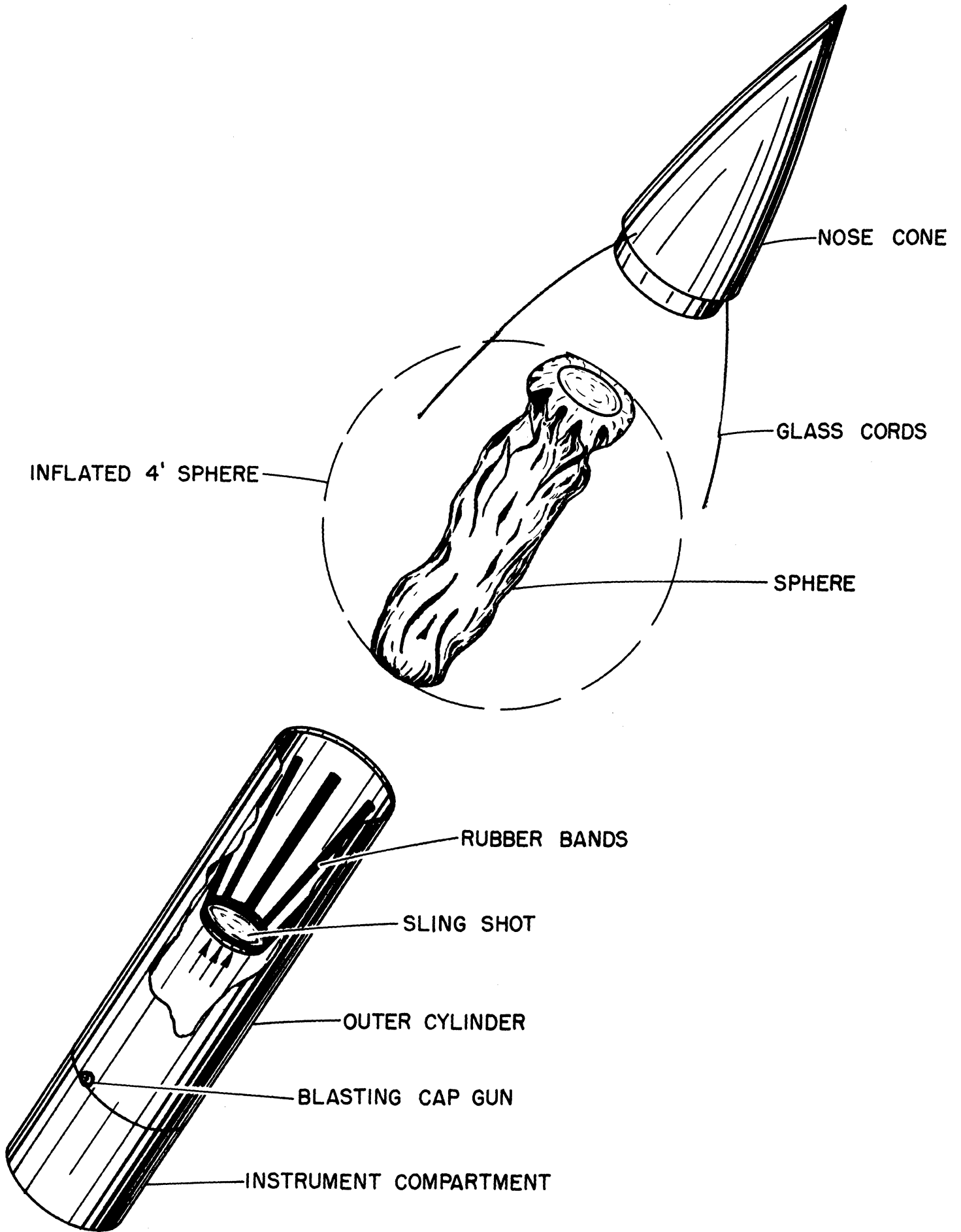


Fig. 5. Ejection System, SC-30.

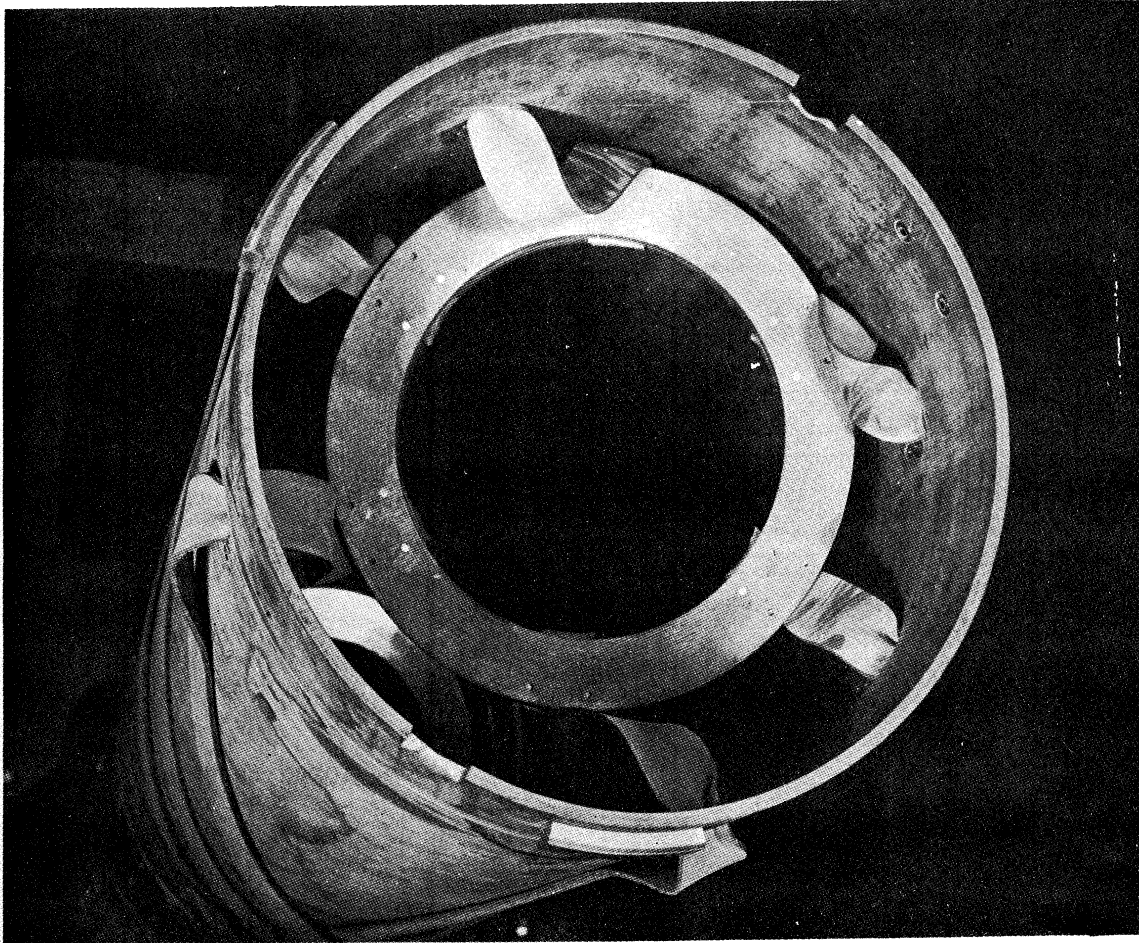


Fig. 6. Sling-Shot Ejector, SC-30.

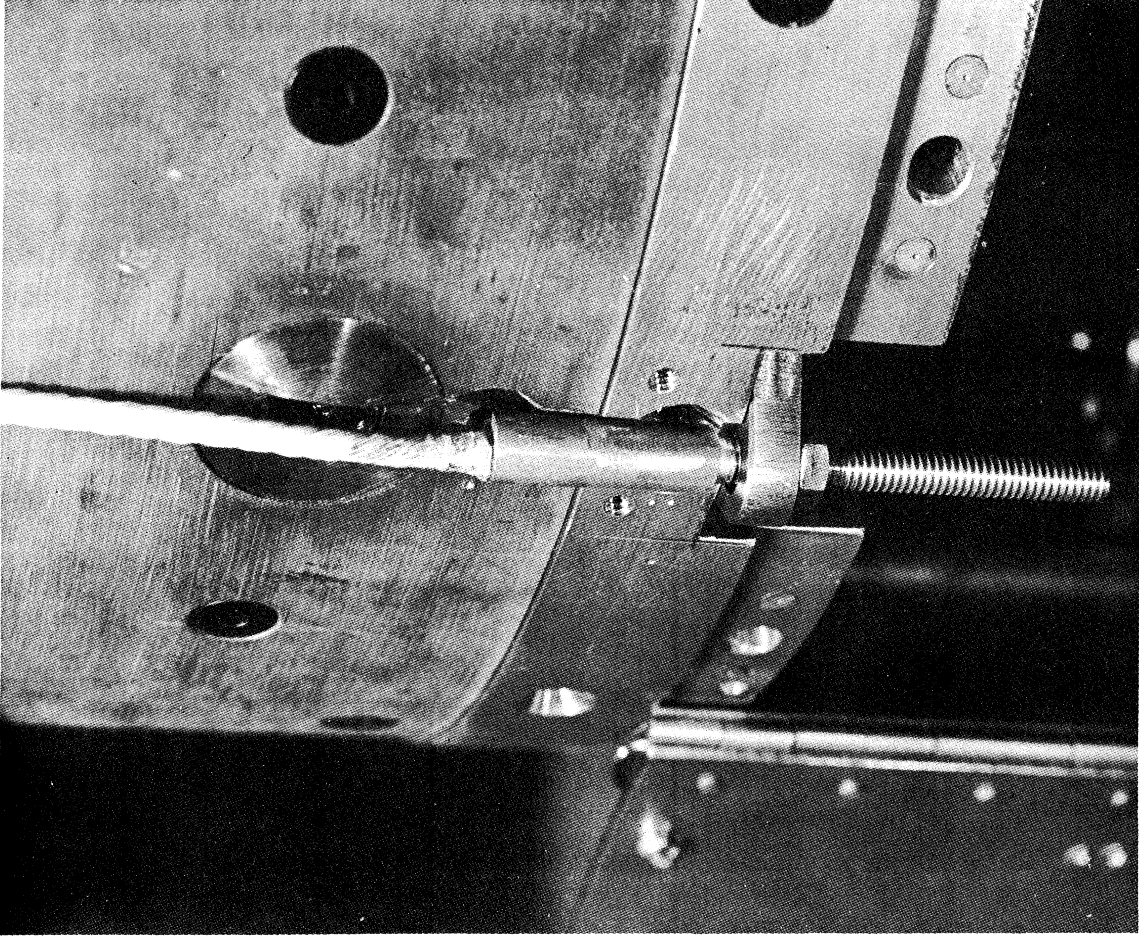


Fig. 7. Fiberglas Cord Tie-Down Detail
and Blasting Cap "Gun," SC-30.

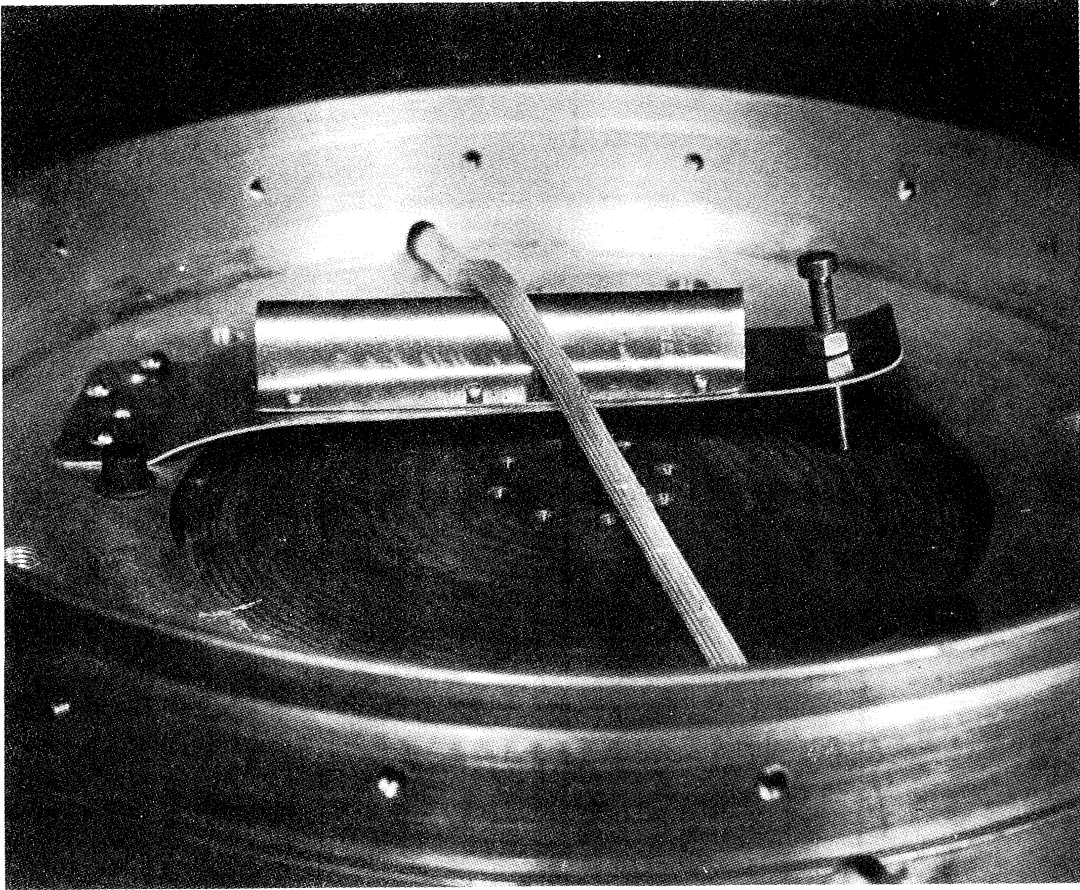


Fig. 8. Hold-Down Lever for Sphere Evacuation Valve, SC-30.

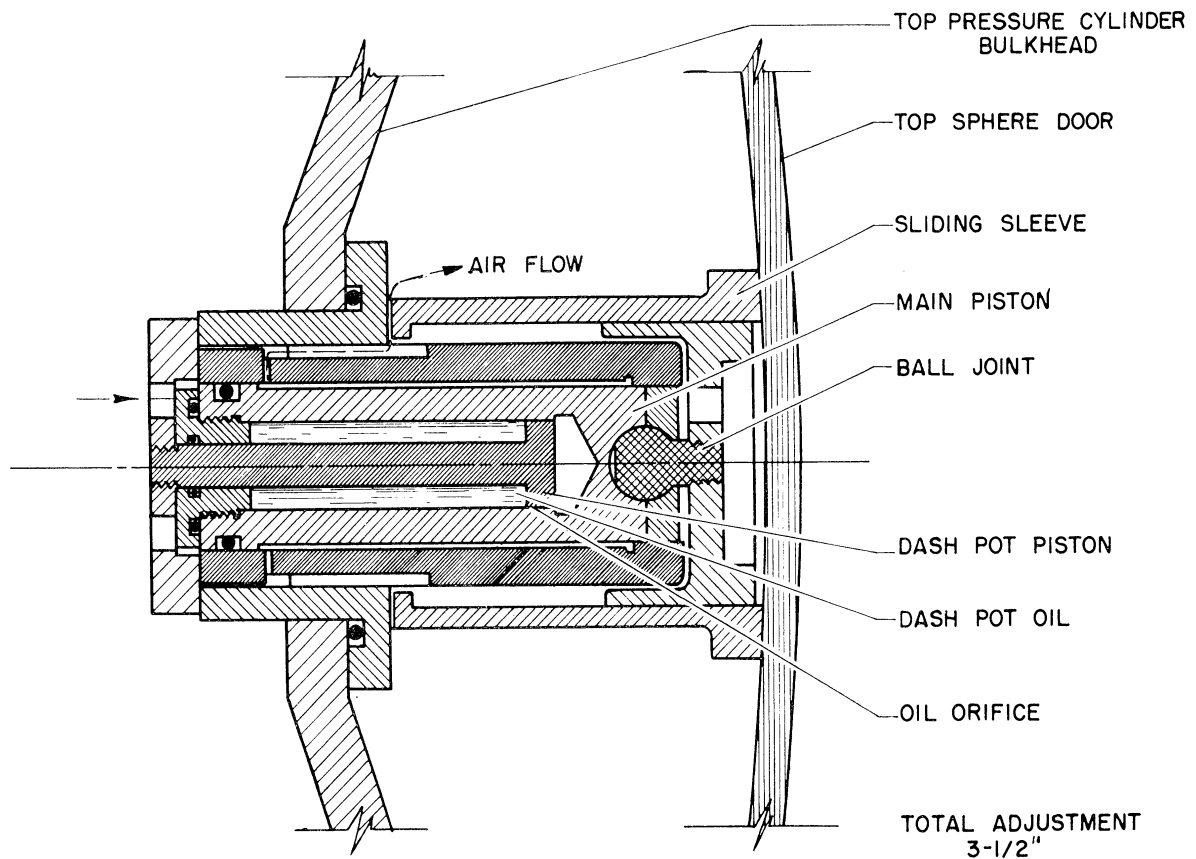


Fig. 9. Revised Sphere Inflation Valve, SC-30.

3.4.2 Ejection Test

Upon completion of the construction of the ejection system, arrangements were made to test it at reduced pressure in a high-altitude chamber at Wright-Patterson Air Force Base, Dayton. Several successful ejections were accomplished during which pressures in the chamber, the sphere, and the inner cylinder were monitored. Fig. 10 shows the instrumentation in position in the chamber prior to sphere ejection. Figs. 11 are pictures from a movie sequence which shows the ejection and inflation of the sphere. Figs. 12 and 13 are plots of the pressure runs. Fig. 12 is a comparison of the internal sphere pressure and the chamber pressure vs. time during "rapid ascent." That is, the chamber pressure was reduced at a rate which approximates the pressure condition of an Aerobee ascent. It is seen that the sphere pressure lag is negligible, thus assuring that the sphere will exhibit no friction due to pressure during ejection from the cylinder. Fig. 13 compares the inner pressurizing cylinder pressure and the sphere pressure in the time interval around ejection and shows the time delay provided by the dash-pot.

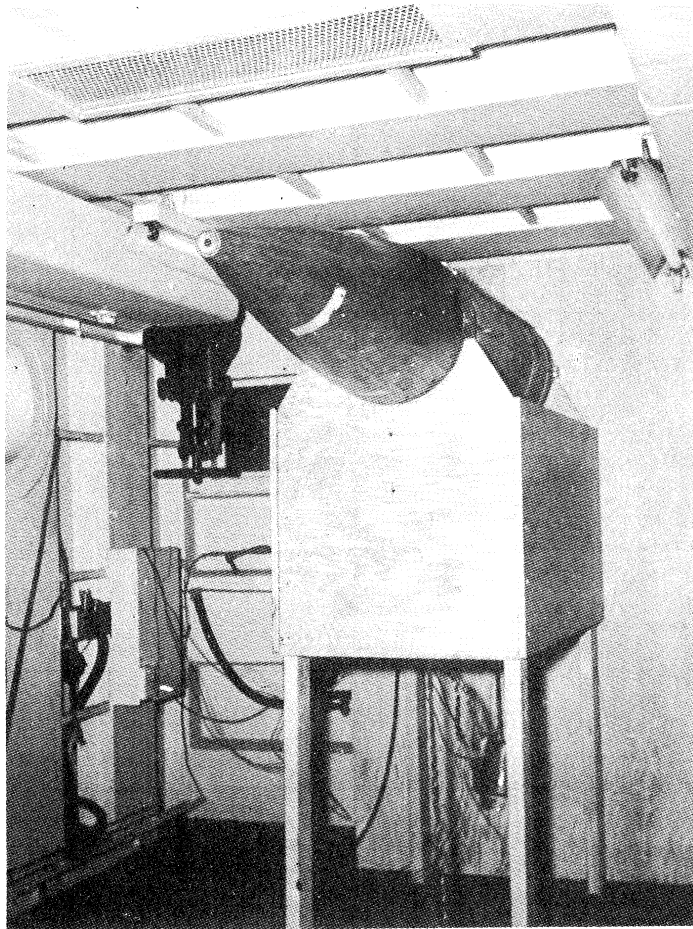


Fig. 10. Test Set-Up, Wright Field, SC-30.

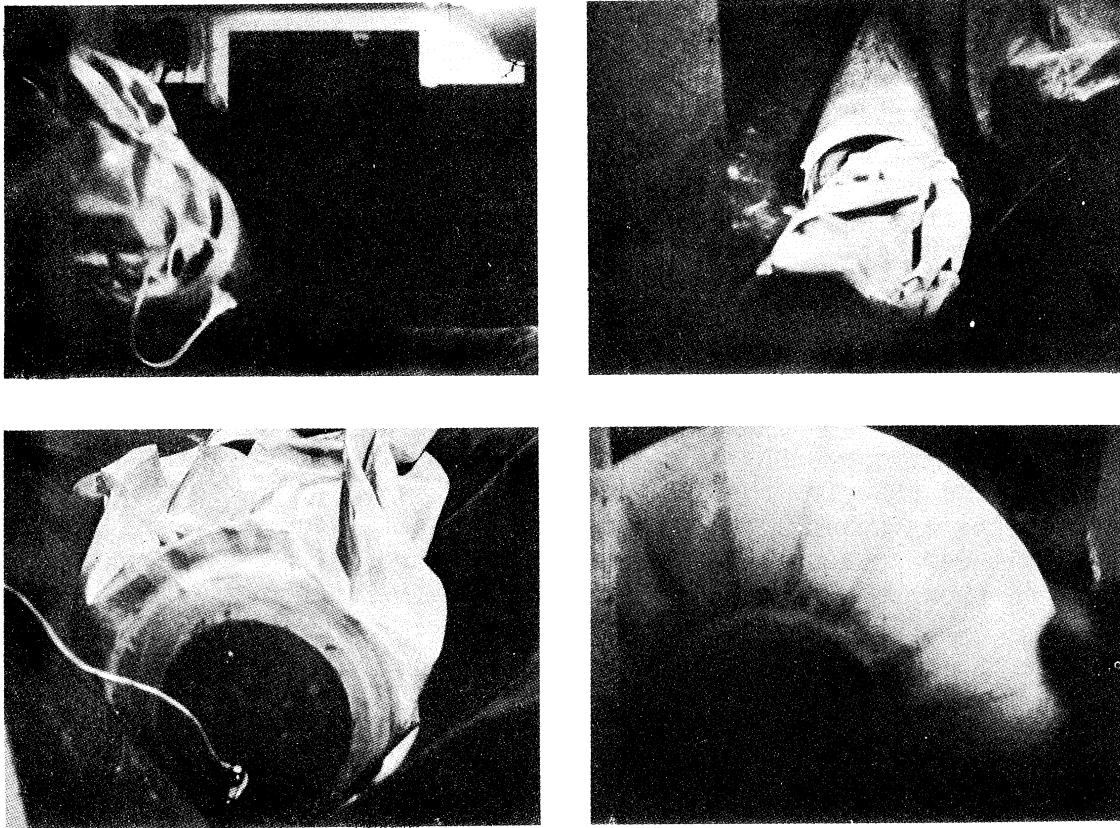


Fig. 11. Sphere Ejection and Inflation, SC-30.

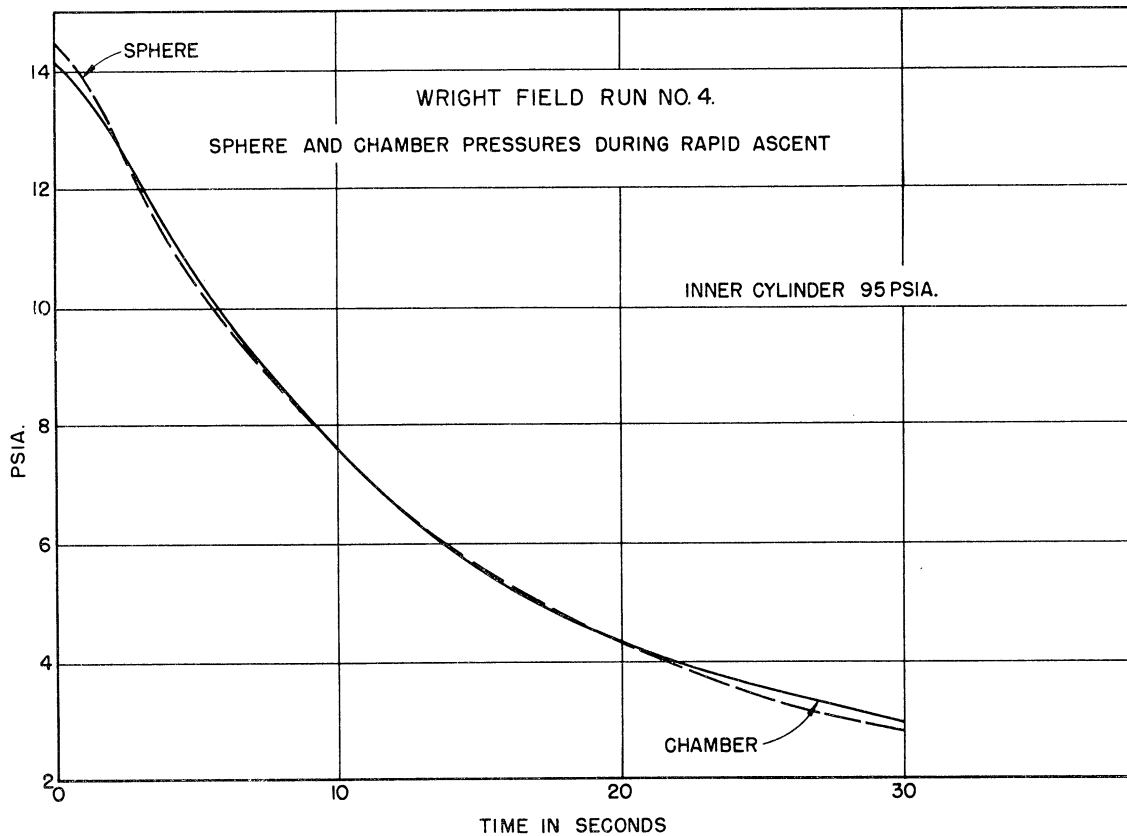


Fig. 12. Sphere and Chamber Pressures, Ejection Test, SC-30.

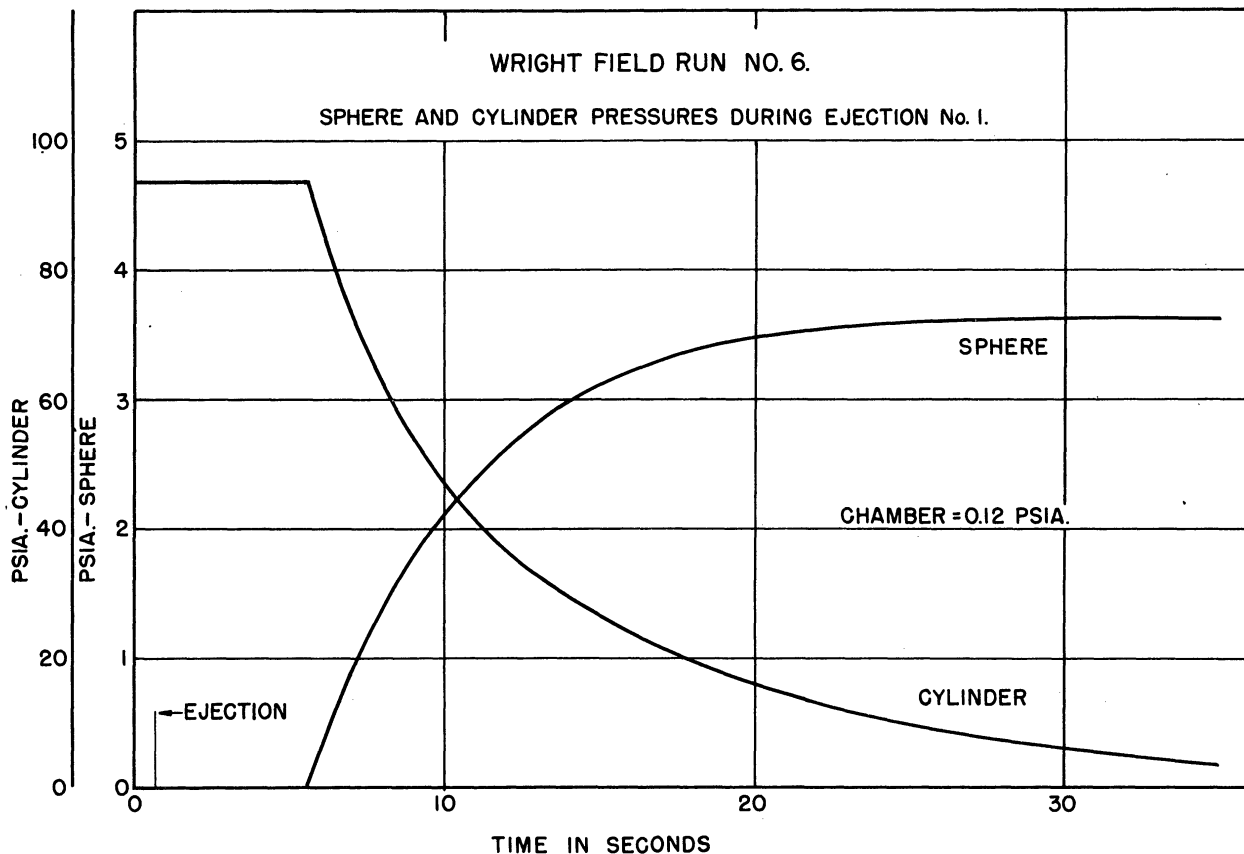


Fig. 13. Sphere and Internal Cylinder Pressures, Ejection Test, SC-30.

3.4.3 Electronics

The circuitry external to the sphere on SC-30 was similar to that of SC-29 with the exception that a radar beacon type AN/DPN-19 (XE-2) was carried. This was included to provide tracking for safety under adverse weather conditions.

The sphere doppler unit used was the one recovered from SC-29. No changes were made. However, in order to reduce the ambiguity of the spin corrections, it was decided to use a single antenna for both doppler frequencies instead of the crossed loops used previously. Fig. 14 illustrates one geometry in which the spin correction for a double loop is ambiguous. With the first figure defining the reference position, it can be seen that a 180° rotation about a horizontal axis reverses the current flow direction (arrows) in both loops A and B with respect to the reference dipole. On the other hand, a 180° rotation about a vertical axis reverses the current direction in A but not in B. This ambiguity would not occur with a single loop.

The development of the single-loop antenna was carried out at Ballistic Research Laboratories. The work is described in the following note received from them.

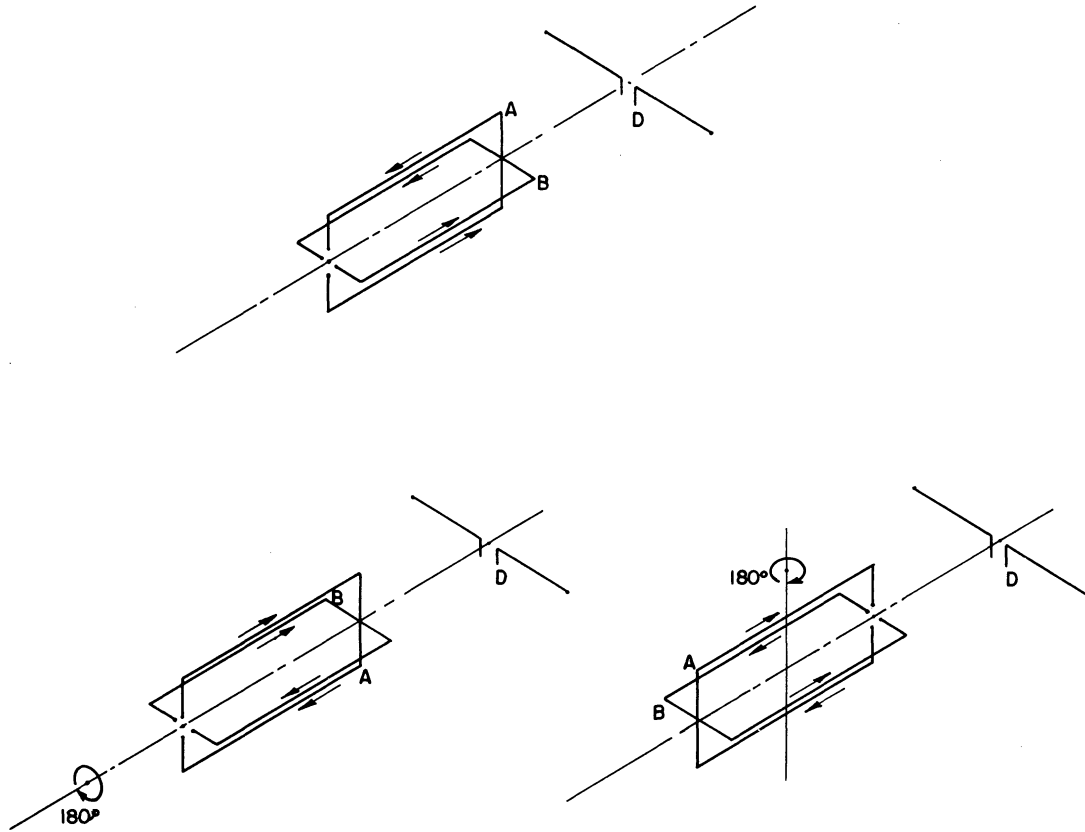
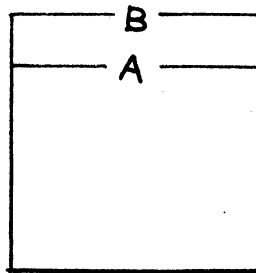


Fig. 14. Spin Ambiguity of Crossed-Loop Antennas.

"PRELIMINARY NOTE ON THE SINGLE-LOOP TWO-FREQUENCY ANTENNA
FOR UNIVERSITY OF MICHIGAN SPHERE PROJECT

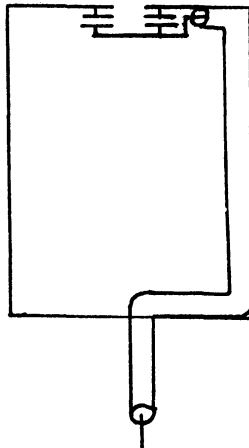
The use of a single loop at two frequencies was requested, and the following is a result of this investigation:



The configuration is as shown above with feedpoint "A" tuned to 37.94 mc and feedpoint "B" tuned to 73.88 mc. Originally, "A" was tuned to 73.88 mc, but the gap capacity transformed by the loop extensions appeared as a shunt capacity across "A." This additional shunt capacity transformed the series resistive component of impedance (approximately 50 ohms) to several hundred ohms. Capacitive matching of inductive loops is only possible when the series resistive component is less than 50 ohms. When feedpoint "B" is used for 73.88 mc, the capacity of "A" has less effect on the circuit because of its lower position along the loop. The transforming done by the extensions when 36.94 mc is used at "A" is not harmful because the loop has a much lower series resistance at this frequency. Consequently, the transformed resistive component is not greater than 50 ohms.

Matching Procedure

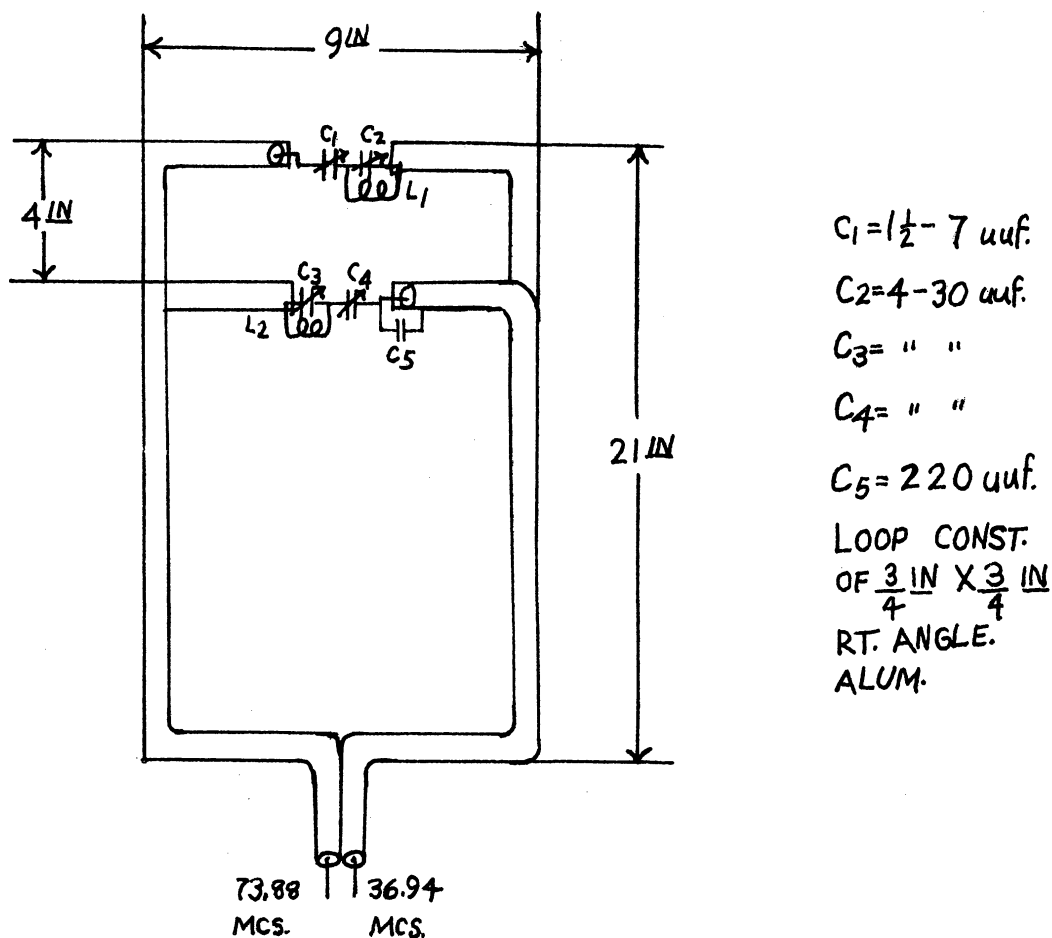
The capacitive matching circuit shown below was used to match each feedpoint separately at its respective frequency with nothing connected to the other feedpoint.



After the approximate values of shunt and series matching capacitors are determined and mounted at their respective feedpoints, the parallel resonant traps are tuned as close as possible to resonance with a Grid Dip Meter and mounted in place (the 74-mc trap at point "A" and the 37-mc trap at point "B"). The Micro-match is placed in series with the coax cable connected to feedpoint "B" and a 74-mc signal source. Readjust series matching capacitor at point "B" for minimum V.S.W.R. The final tuning of the 74-mc trap at feedpoint "A" is accomplished by varying the parallel capacitor in the trap circuit a small amount (enough to cause a mis-match of 2 to 1 in V.S.W.R.), then readjusting the series matching capacitor at point "B" for minimum V.S.W.R. The series matching capacitor at point "A" is then rotated through its entire range noting the amount of mis-match it causes. This procedure is repeated until the series matching capacitor at point "A" has no effect on the match at 74 mc. This is a critical adjustment, but the trap can be "walked" into resonance by several trials using the above procedure. It may now be necessary to change the value of the shunt matching capacitor at point "B" (74-mc feedpoint) to obtain the desired V.S.W.R. This will not change the tuning of the trap. The same procedure is used to tune the 37-mc trap. Finally, the series matching capacitor at the 74-mc feedpoint is readjusted for minimum V.S.W.R. at 74 mc. This is necessary because in the original tune-up the 37-mc trap in series with this capacitor was not tuned; consequently, the series reactance was slightly different.

The complete circuit for the two-frequency loop is shown below. A balanced system was formed by attaching the feed cables along the sides of the loop.

The cross-coupling between the loops was measured by connecting 37-mc or 74-mc signal source to the respective antenna feedpoints and measuring the amount of signal from the other feedpoint with an F.S. Meter. With a 0.1 V, 74-mc signal source connected to the 74-mc feedpoint, the signal out of the 37-mc feedpoint was .095 V which amounts to 27 db of isolation. With a 0.2V, 37-mc signal source connected to the 37-mc point, the signal out of the 74-mc point was .093 V which amounts to 20 db of isolation.



The loss of the traps was measured by using an F.S. Meter and a small coupling loop placed about three feet from the antenna. The reference field strength was measured with all traps removed from the circuit and the antenna matched at 74 mc. It was necessary to completely disconnect the trap circuits and remove them from the antenna as coupling was experienced when the traps were in the field with no direct connection. The traps were then added one at a time, rematching as every change was made and keeping the input power constant.

At 74 mc, the loss in the trap circuit was 3 db. This was due entirely to the 74-mc trap circuit. It is difficult to obtain the "Q" necessary to obtain a parallel impedance higher than the loop impedance.

At 37 mc, the loss in the trap circuits was 4-1/2 db of which 1-1/2 db was due to the 37-mc isolating trap and 3 db due to the 74-mc trap in series with the loop.

The resistive component of the terminal impedance is very low in the order of 2 or 3 ohms, and the resistive component of the 74-mc trap is of comparable resistance. Reducing the number of turns to lower the resistive component unfortunately also reduces the trap's effectiveness at 74 mc, so a compromise value was used."

Fig. 15 shows the completed antenna mounted on the lower bulkhead of the Fiberglas air cylinder inside of which the antenna is mounted. The smaller loop is the receiving antenna. Also mounted on the bulkhead is a 0-110 psia Giannini model 46118D-A-11-20 pressure gage for monitoring the air cylinder pressure prior to flight.

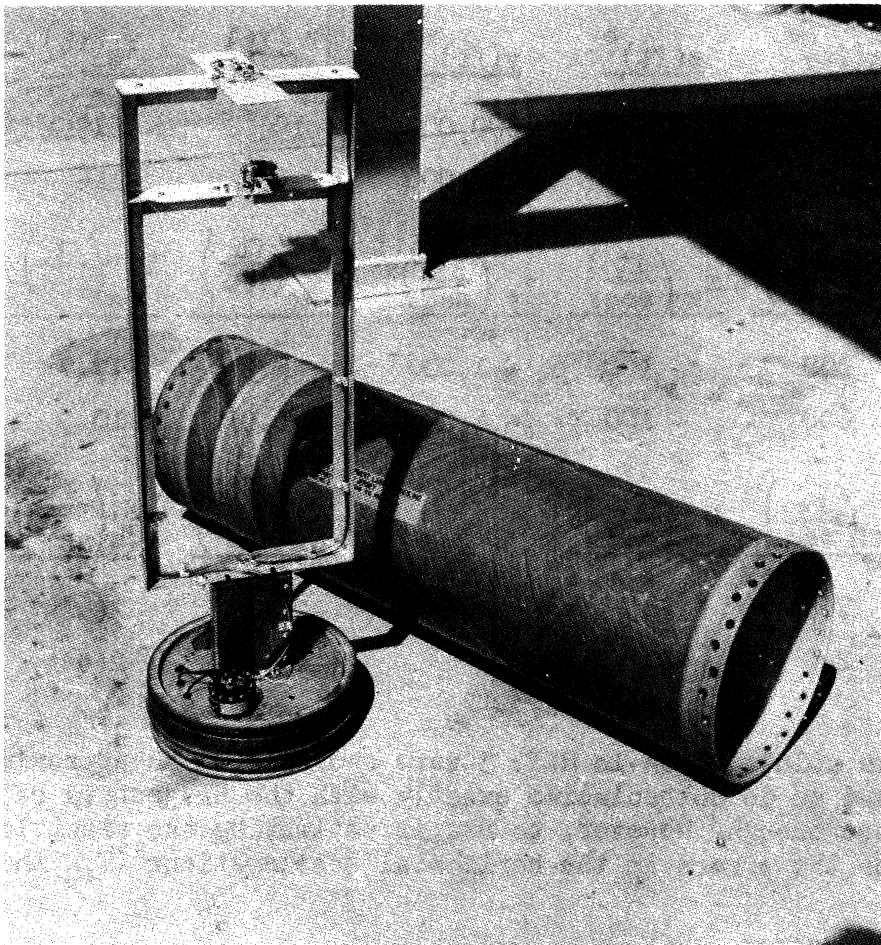


Fig. 15. Single Doppler Antenna, SC-30.

3.5 Large Sphere for Measuring Winds

Several variations of the sphere experiment have been considered, particularly with reference to the possibility of measuring winds. It was thought that a large diameter, light weight sphere might be tracked with sufficient precision to give useful information on wind velocities and directions. As a first step, information on the precisions of some currently operating applicable tracking systems were obtained. Next, the trajectory of a large, light sphere was predicted, first by manual calculation and then on an analog computer.

Estimates of the precision of several currently or about-to-be available tracking systems were examined. The systems considered are either in operation at, or proposed for, the WSPG-Holloman range and include DOVAP, MIRAN, single radar, chain radar, and optical. A rigorous comparison of defined precision indices for all parts of a trajectory is not possible with the data available. However, the following generalization may be made: the DOVAP system is at least one order of magnitude more precise than any of the other systems listed above.

For the purpose of evaluating the large-sphere experiment, the following values³ for the maximum errors (T) and the probable errors (P) of the DOVAP system for various points on a trajectory were used:

Point	$x(\text{ft})^*$	$z(\text{ft})^*$	$y(\text{ft})^*$	$T_x(\text{ft})$	$T_z(\text{ft})$	$T_y(\text{ft})$
B	110,000	-20,000	300,000	192	413	75
E	75,000	0	100,000	67	144	42
	$v_x \left(\frac{\text{ft}}{\text{sec}} \right)$	$v_z \left(\frac{\text{ft}}{\text{sec}} \right)$	$v_y \left(\frac{\text{ft}}{\text{sec}} \right)$	$T_{v_x} \left(\frac{\text{ft}}{\text{sec}} \right)$	$T_{v_z} \left(\frac{\text{ft}}{\text{sec}} \right)$	$T_{v_y} \left(\frac{\text{ft}}{\text{sec}} \right)$
B	600	- 100	- 1,000	8.3	17.7	3.5
E	600	- 100	- 4,000	5.0	10.5	1.9
	$T_v \left(\frac{\text{ft}}{\text{sec}} \right)$	$P_v \left(\frac{\text{ft}}{\text{sec}} \right)$		$T_{a_x} \left(\frac{\text{ft}}{\text{sec}^2} \right)$	$T_{a_z} \left(\frac{\text{ft}}{\text{sec}^2} \right)$	$T_{a_y} \left(\frac{\text{ft}}{\text{sec}^2} \right)$
B	7.5	4.7		2(est)	2(est)	1.1
E	2.0	1.3		2(est)	2(est)	1.4

The points given in Ref. 3 were chosen from an approximate Aerobee trajectory and so do not coincide exactly with the trajectory of a sphere. They are close enough, however, to use in estimating the precision of tracking. No values for the errors in the horizontal accelerations (T_{a_x} and T_{a_y}) were

* x positive north, z positive east, y positive upward.

computed in Ref. 3. The value 2 ft/sec^2 is estimated as being of the right order of magnitude since the maximum error in the general transmitter-to-sphere-to-receiver distance (T_{au}) is given as 2 ft/sec^2 (Ref. 3). It should be noted that these errors are for a non-spinning missile and may be as much as four times larger with spin. On the other hand, improvement by a factor of 2 or 3 may be gained from smoothing.

Fig. 16 is a plot of the vertical and horizontal velocities and horizontal acceleration of a freely falling sphere ten feet in diameter and weighing ten pounds. The calculations were made manually using UARRP densities and an assumed unidirectional wind velocity profile varying linearly from 184 feet per second at 150,000 feet to 400 feet per second at 300,000 feet. This particular wind profile is unrealistic because it is known that upper air winds change direction. Thus a sphere would experience somewhat larger accelerations than shown in Fig. 16 when the sphere and wind velocities were not in the same direction. These accelerations would increase appreciably as the density increased, that is, the accelerations would not decrease below 230,000 feet as in the special case of Fig. 16. Very roughly, then, the acceleration of such a sphere, and consequently the wind velocity,⁴ could be measured to $\pm 50\%$ at 230,000 feet. The precision would improve with decreasing altitude.

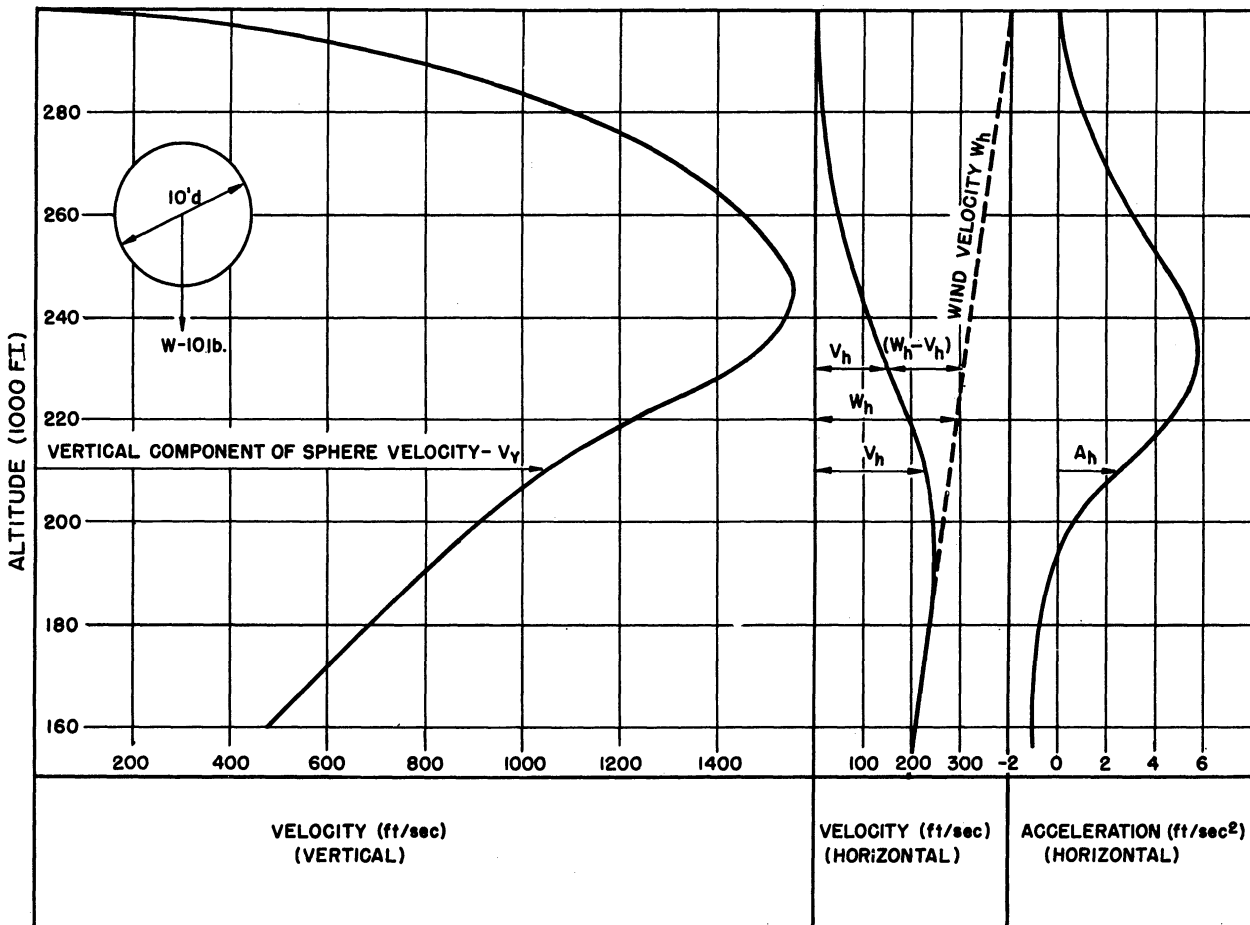


Fig. 16. Large-Sphere Trajectory.

This evaluation is quite incomplete. It is necessary to predict motions for much more complicated wind structures and for spheres whose weight to area ratios are more favorable. This involves a considerable amount of calculation. In order to make rapid comparisons the trajectories may be run off on a computer. As a first step the problem of Fig. 16 was set up⁵ on a Reeves REAC model C 101 analog computer and the result checked with good agreement. Further trajectories will be computed.

3.6 References.

- (1) The Rocket Panel, Phys. Rev., 88 (1952), p. 1027.
- (2) Navord Report 2352, 14 August 1952.
- (3) Ballistic Research Laboratories, Tech. Note No. 292, p. 5, 1950.
- (4) Liu, V. C., Univ. of Mich. ERI Proj. 2000 Memo. No. 3, Eq. 10, p. 3, 1951.
- (5) ARC-ERI, Univ. of Mich. External Memo. No. 28, 1949.

4. SAMPLING

4.1 Sample Analysis

The results of analyses of three more sample bottles were received from Professor Paneth:

<u>Bottle</u>	<u>Mean Altitude km MSL</u>	<u>Amount of Sample cc NTP</u>	<u>Analysis (a)</u>			
			<u>Oxygen</u>	<u>Helium</u>	<u>Neon</u>	<u>Argon</u>
C-3 ^(b)	93.3	0.0026	0	--	--	0.82
C-1 ^(b)	88.4	0.012	0	2.943	1.395	0.82
B-18-P ^(c)	ground	0.134	0	0.997	1.003	0.99

Vol. ratio to N₂ in sample

(a) $\frac{\text{Vol. ratio to N}_2 \text{ in sample}}{\text{Vol. ratio to N}_2 \text{ in ground air}}$

Mean deviations based on a few runs usually less than ± 0.005 .

(b) From V-2 59 fired 20 May 1952.

(c) "Vial" type control bottle. See P.R. 3, p. 8.

These results are similar to those given in the previous report. The two highest bottles analyzed so far are C-3 and C-1. The latter shows the greatest separation yet measured.

4.2 Sampling Aerobee SC-31

Because of the negative results of the analyses of control bottles B-17-P and B-18-P, it was felt that selective adsorption and "static orifice selection" were tentatively eliminated as causes of separation in upper-air bottles. A dynamic selection phenomenon remains as the only suggested source of separation to be investigated. Three methods of investigating whether or not such a phenomenon is present in rocket sampling were mentioned in the previous report. It was thought that sampling at peak at subsonic velocity would be most conclusive but difficult to engineer. Therefore, it was decided to employ the second-best alternative, that of sampling with orifices of three different sizes.

The advantages of peak-sampling and methods of handling the design problems were reconsidered, and it was finally decided that the method is feasible. The problem is to detach a pressure-tight canister containing the sample bottles from the rocket and nose cone so that during sampling at peak it is not outgassing and is far removed from all other parts of the rocket. Design of the apparatus to accomplish this was started. The scheme, shown in Fig. 17, uses the thrust of a T-31 Jato to accomplish the separation. At the instant the Jato is fired, on the upward leg, the lower part of the canister is separated from the rocket. Half way through the one-second burning time of the Jato, the nose cone is separated from the upper part of the canister.

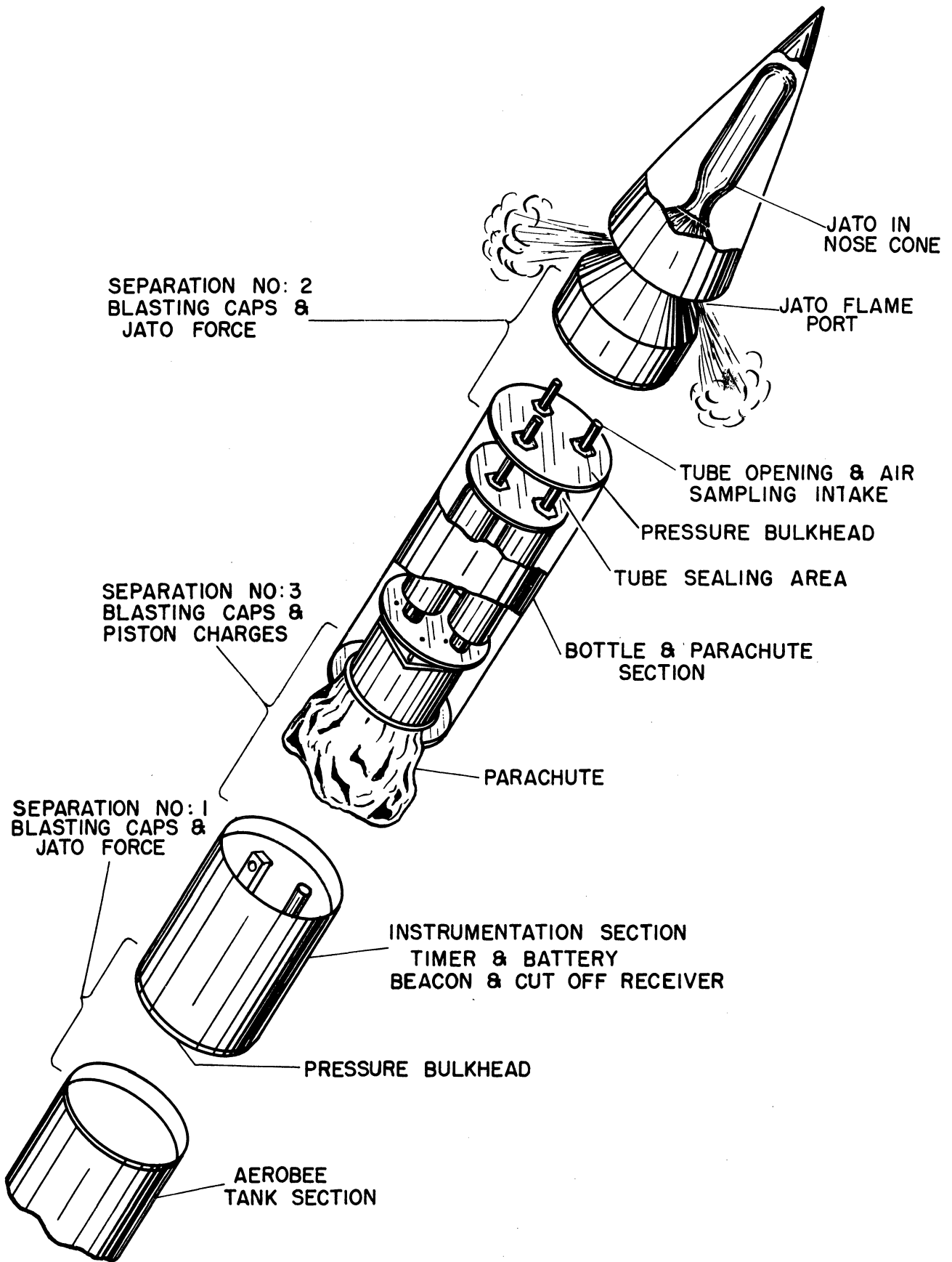


Fig. 17. Sampling Aerobee SC-31.

By the time peak is reached the rocket, canister, and nose-cone are separated in space by several thousand feet. Finally, on the down-leg the parachute section is separated, releasing the parachute and separating the beacon, timer, and cut-off receiver section, leaving the bottles as the parachute drop-load. The three separations are accomplished in each case using the standard parachute separation rings used successfully on several previous Michigan Aerobees. The first is initiated by cut-off receiver command, the second and third by timer.

Two components, originally necessary for the three-size orifice Aerobee will be described, although neither is essential in the peak-sampling technique. The first, a sealer for sealing 2-inch diameter copper tubing will be used in SC-31 because of the shorter filling time-constant. Seals made in 2-inch tubing with an experimental set of jaws are shown in Fig. 18. Pressure was applied in a Tinius-Olsen Testing Machine, and the seals were found to be vacuum tight. Fig. 19 illustrates the design of the flight sealer. It will be constructed of Hy-Ten steel throughout and has a bore of 3 inches. It is designed to use 16 grams of black powder, which will develop 20,000 plus pounds total force.

The second component originally necessary for SC-31, an aspect camera, will not be used. However, it is described because of other possible applications. The characteristics of cameras⁽¹⁾ used for measuring aspect on previous rockets were compared with those of commercially available cameras. The Robot-Star remotely operated sequential exposure camera, manufactured by the Robot-Berning Company, appeared to have possibilities. The camera is equipped with an f 1.9 lens and 1/500-second shutter. It uses 35-mm film wound through by a spring motor giving 55 1-inch x 1-inch exposures. The film wind is triggered by a solenoid operating on 12 to 18 volts DC. The camera was mounted on a rotating table, and pictures of a grid were taken at various rotational speeds. Fig. 20 shows the grid taken with the camera stationary and then rotating at 1 rps. Since this is a typical roll-rate for an Aerobee, it was concluded that pictures of sufficient clarity for measuring the angle of attack could be obtained.

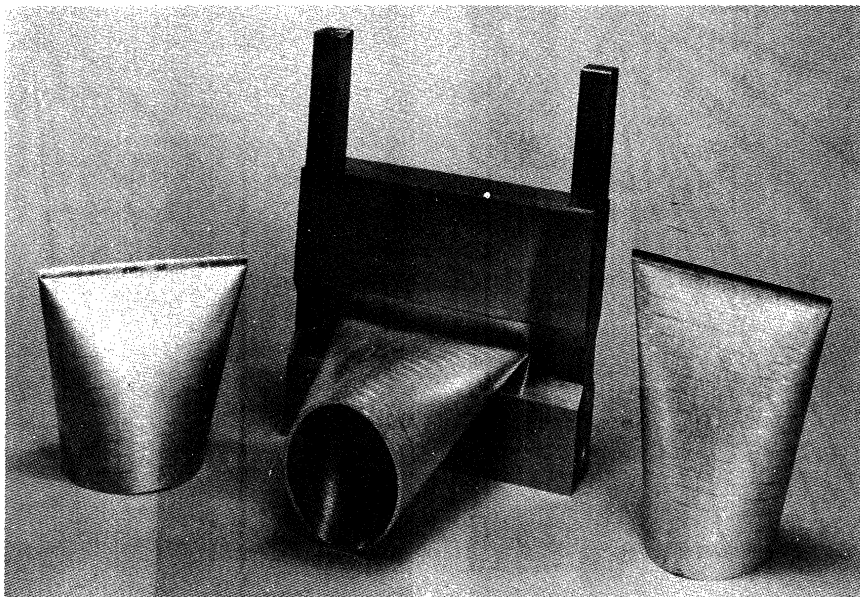


Fig. 18. Seals in 2-Inch Copper Tube.

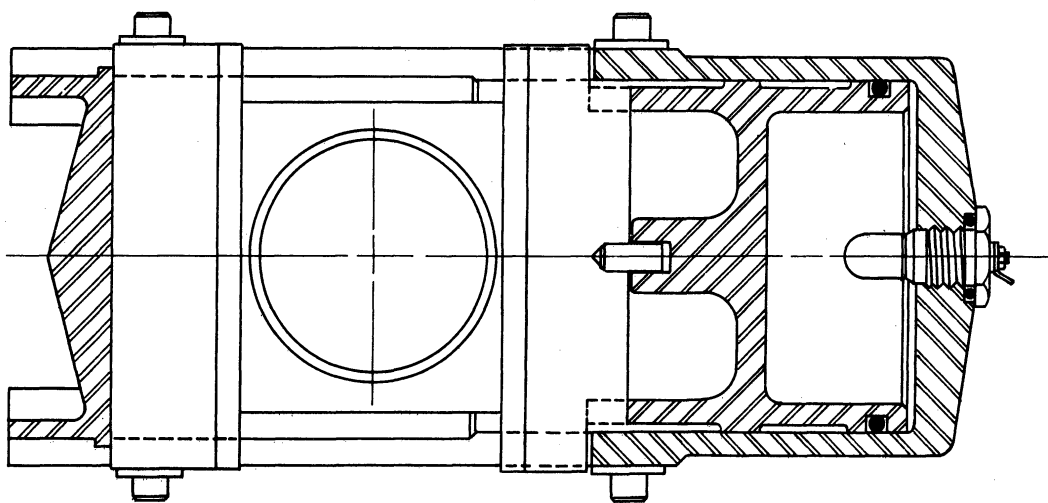
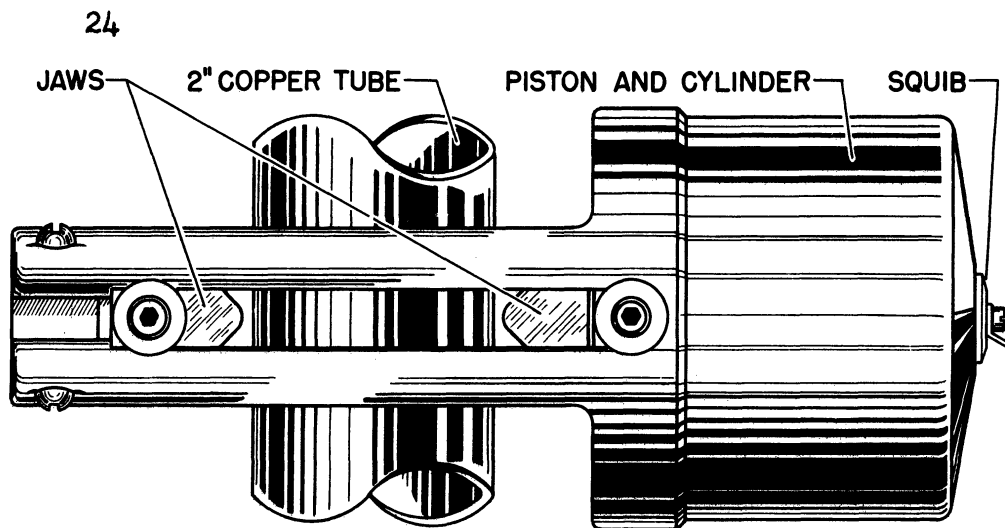


Fig. 19. The 2-Inch Pyrotechnic Sealer for Flight, SC-31.

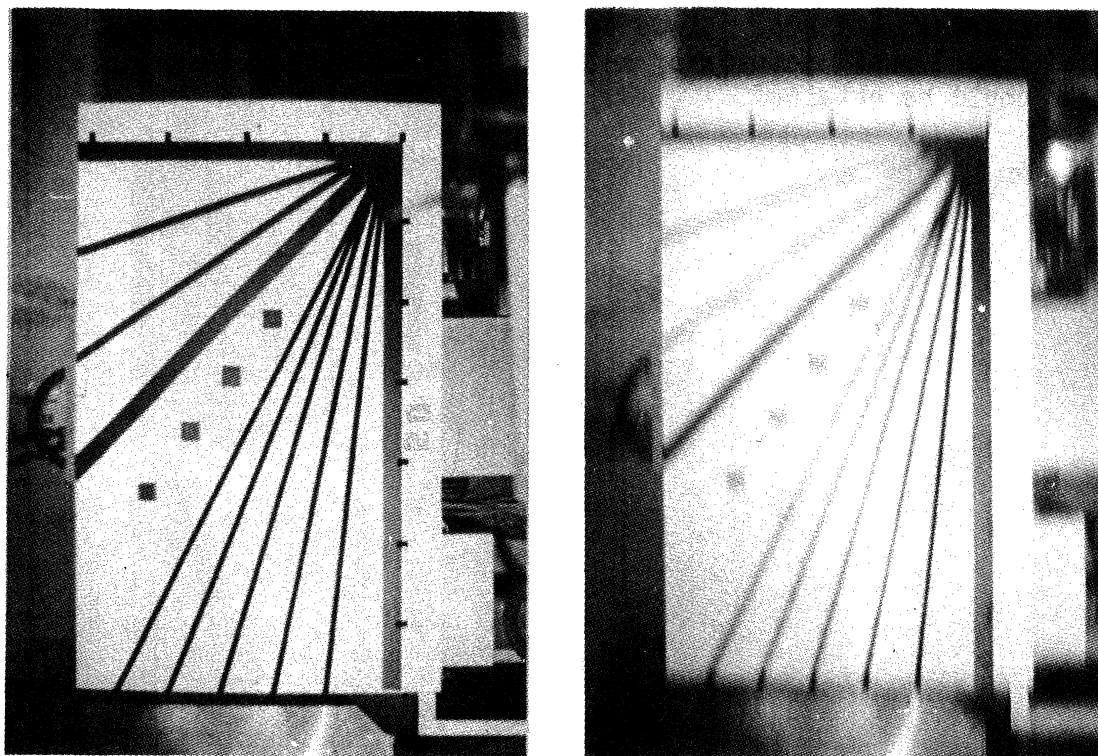


Fig. 20. Pictures Taken with Robot-Star Camera.

4.3 Miscellaneous

A control bottle containing ground air was prepared for Dr. M. Dole at Northwestern for use in his work with oxygen isotopes.⁽²⁾ After preparing, evacuating, and sealing the bottle by standard methods, the ground-air vial was broken inside and the pressure monitored. The sample was then transferred into three glass vials for shipment to Dr. Dole.

Investigation of nickel-ribbon Piranis for monitoring bottle pressures was started. Both AC and DC calibration circuits were used. Preliminary results indicate improved sensitivity over platinum wire in the pressure region 1-10 μ Hg.

4.4 References

- (1) Holliday, C. T., "Preliminary Report of High Altitude Photography," Photographic Eng., 1 (1950), p. 16.
- (2) University of Michigan, ERI Project 2000, Quarterly Report No. 3 (1952), p. 11.

5. CORRECTION

In Progress Report No. 3, Quarterly Report for the period July 1, 1952, to September 30, 1952, page 17, equation (7) should read:

$$p \approx p_2 = \frac{1}{2} \left(\frac{4\gamma}{\gamma+1} \right)^{\frac{\gamma+1}{\gamma-1}} (4\gamma)^{\frac{1}{1-\gamma}} \frac{P}{V^2} \left\{ 1 - \frac{\gamma-1}{2P} \left[\int_{h_0}^h \frac{P}{V^2} g \, dh + 2 \left(\frac{\gamma+1}{4\gamma} \right)^{\frac{\gamma+1}{\gamma-1}} (4\gamma)^{\frac{1}{\gamma-1}} p_0 \right]^{\frac{1}{\gamma-1}} \right\}.$$

6. REPORTS ISSUED AND LABORATORIES VISITED

No reports were issued during the period. The following places were visited during the course of the work:

Ballistic Research Laboratories
Evans Signal Laboratory
Goodyear Tire and Rubber Company
Wright-Patterson Air Force Base
Young Development Company

7. FUTURE PROGRAM

Sphere Aerobee SC-30 will be fired. The data from sphere Aerobee SC-29 will be reduced. Preparation of sampling Aerobee SC-31 will continue. The investigation of possible sources of separation in upper-air samples other than by upper-air phenomena will continue.

8. ACKNOWLEDGMENT

Thanks are due the Meteorological Branch of the Signal Corps for cooperation and support and to Ballistic Research Laboratories for continued cooperation in the sphere experiment. We are again indebted to the Aero-Medical Laboratory at Wright Field for use of the high altitude chamber. Figs. 6, 7, and 8 are Signal Corps photographs.

UNIVERSITY OF MICHIGAN



3 9015 03023 1891